ISSN 2176-5480

22nd International Congress of Mechanical Engineering (COBEM 2013)
November 3-7, 2013, Ribeirão Preto, SP, Brazil

FLOW OF ELASTO-VISCOPLASTIC FLUIDS INSIDE A CAVITY

Daniel D. dos Santos
Giovanni M. Furtado
Sergio Frey
Federal University of Rio Grande do Sul
dallonder@mecanica.ufrgs.br,giovannimf@mecanica.ufrgs.br,frey@mecanica.ufrgs.br

M. F. Naccache
P. R. de Souza Mendes
Pontificia Universidade CatÃşlica do Rio de Janeiro
naccache@puc-rio.br, pmendes@puc-rio.br

Abstract. *The elastic behavior of viscoplastic fluids is analyzed numerically, using a novel constitutive model. The equation predict not only elasticity but also the thixotropic behavior of viscoplastic fluids, and is based on the Oldroyd-B model - but with variable viscosity, relaxation and retardation times. These parameters depend on the material microstructure, which level is described by a structure parameter. The performance of the constitutive model is evaluated in the leaky cavity problem, using the finite element technique, and a Galerkin least-squares-type model. Stress, velocity, and strain-rate fields are obtained in order to clarify the role of elasticity and yield stress on the flow. Moreover, the results are compared to previous ones, obtained with a simpler constitutive equation, in order to evaluate the capabilities and advantages of the constitutive equation.*

Keywords: *viscoplastic fluids, elasticity, yield stress 3…*

1. INTRODUCTION

Elastic and viscous effects in the inertialess flow of elasto-viscoplastic fluids inside a lid-driven cavity are analyzed in the present work. This class of materials can be present in several important industrial sectors – such as oil, food, pharmaceutical, and cosmetics. The main characteristic of the viscoplastic fluids is that below the "yield stress" they are highly structured materials with very high viscosities. When submmited to stresses above the yield limit their structure breaks, a deep viscosity decay occurs and they behave as purely viscous fluids, with constant or shear thinning viscosity. Due to the very low deformations that these fluids experience below yield stress, several works in the literature report that these materials behave as solid materials at this range of stresses ((Barnes, 1999a), (Barnes, 1999b)). However, more recently, with the development of more precise measurement techniques, it is observed that there may be some deformation below the yield limit (e.g. (Carter and Warren, 1987), (de Souza Mendes *et al.*, 2007), (Sikorski *et al.*, 2009)). There are also several experiments showing that elasticity can be present in this range of stresses ((de Souza Mendes *et al.*, 2007), (Sikorski *et al.*, 2009)).

Viscoplastic fluids can present elasticity and thixotropy. Recently, an Oldroyd-B type constitutive equation was proposed by (de Souza Mendes, 2009) to model the behavior of elasto-viscoplastic fluids, and also thixotropy. The equation involves the determination of a structure parameter to describe the fluid microstructure, with the aid of an aditional equation that has to be solved together with the conservation and constitutive equations.

Many works in the literature present numerical studies of viscoplastic fluid flows with no elasticity or thixotropy (e.g. (Alexandrou *et al.*, 2001b); (Alexandrou *et al.*, 2001a); (Alexandrou *et al.*, 2001a); (Besses *et al.*, 2003); (Burgos and Alexandrou, 1999); (Burgos *et al.*, 1999); (Mitsoulis *et al.*, 2006); (Naccache and Barbosa, 2007); (Mitsoulis *et al.*, 1993); (Hammad *et al.*, 2001); (Liu *et al.*, 2002); (Zisis and Mitsoulis, 2002); and (Roquet and Saramito, 2003)). All these works neglected inertia effects, and employed regularized equations proposed by (Papanastasiou, 1987), by (Bercovier and Engelman, 1980) or by (de Souza Mendes and Dutra, 2004)) to model fluid viscosity. Regarding thixotropy and elasticity, there are not so many works that consider this kind of behavior either because modeling is still a challenge, or because of the lack of experimental data ((Barnes, 1997); (Mewis, 1979); (Mewis and Wagner, 2009), (de Souza Mendes and Thompson, 2012a)). (Saramito, 2007) presented a new three-dimensional model for elasto-viscoplasticity based on both Bingham and Oldroyd-B fluid models, obtaining good results in the study of simple flows. (Sofou *et al.*, 2008) obtained experimentally the rheology of bread dough, and used two equations to model the fluid, the Herschel-Bulkley equation to describe the viscosity of the flour dough and the K-BKZ model with a yield stress, to represent the stress relaxation and the viscoelastic nature of the material. (Nassar *et al.*, 2011) employed an elasto-viscoplastic model to simulate an expansion-contraction axisymmetric flow, comparing the results with experimental data from the literature. Using the same equation, (Martins *et al.*, 2013) solved the lid-driven cavity problem, with good qualitative results. (de

Souza Mendes, 2009) improved the latter model using a microstructure parameter that gives the level of the structure breakage of a viscoplastic material – function of the stress level applied to the material. In this equation, thixotropy is also taken into account, and the relaxation time and viscosity are functions of the structure level of the material. Further on, (de Souza Mendes, 2011) extended this model to an Oldroyd-B type model.

In this work, we solve the lid-driven cavity problem with the constitutive equation proposed by (de Souza Mendes, 2011), using a three-field Galerkin least-squares (GLS) finite element formulation. The formulation is able to successfully capture the elastic and viscous effects present in the current model, even making use of an equal-order combination of linear Lagrangian finite elementinterpolations. The role of elasticity, yield stress, shear-thinning and kinematics oin the flow pattern are presented and discussed.

2. MECHANICAL MODELING

The mass and momentum conservation equations for steady creeping flow are given by:

$$\nabla \cdot \boldsymbol{u} = 0 \tag{1}$$

$$\nabla P - \nabla \boldsymbol{\tau} = 0 \tag{2}$$

where $\boldsymbol{u}$ is velocity vector, $P = p + \rho\phi$ is the modified pressure, p is the pressure, ρ is the fluid density, and $\boldsymbol{g} = -\boldsymbol{\nabla}\phi$ is the gravitational force per unit mass. To model the elasto-viscoplastic behavior of the fluid, the extra-stress tensor $\boldsymbol{\tau} \equiv \boldsymbol{T} + p\mathbf{1}$ is described by:

$$\boldsymbol{\tau} + \theta_1 \overset{\triangledown}{\boldsymbol{\tau}} = \eta \left(\dot{\boldsymbol{\gamma}} + \theta_2 \overset{\triangledown}{\dot{\boldsymbol{\gamma}}} \right) \tag{3}$$

where $\dot{\boldsymbol{\gamma}} \equiv \nabla \boldsymbol{u} + \nabla \boldsymbol{u}^T$ is the rate of deformation tensor field, and the upper-convected time derivatives of $\boldsymbol{\tau}$ and $\dot{\boldsymbol{\gamma}}$ are given by

$$\overset{\triangledown}{\boldsymbol{\tau}} \equiv \frac{d\boldsymbol{\tau}}{dt} - \boldsymbol{\tau} \cdot \nabla \boldsymbol{u} - \nabla \boldsymbol{u}^T \cdot \boldsymbol{\tau} \tag{4}$$

and

$$\overset{\triangledown}{\dot{\boldsymbol{\gamma}}} \equiv \frac{d\dot{\boldsymbol{\gamma}}}{dt} - \dot{\boldsymbol{\gamma}} \cdot \nabla \boldsymbol{u} - \nabla \boldsymbol{u}^T \cdot \dot{\boldsymbol{\gamma}} \tag{5}$$

where $d(*)/dt \equiv \partial(*)/\partial t + \boldsymbol{u} \cdot \nabla(*)$ is the material time derivative.

The rheological parameters appearing in the constitutive equation, namely the viscosity function η, and the relaxation and retardation times θ_1 and θ_2, respectively, are functions of the structure parameter λ, which evolves with the time that the fluid is being submitted to a certain stress. The time-dependent (thixotropic) behavior is expressed by an evolution equation for the structure parameter, given by:

$$\frac{d\lambda}{dt} \equiv \frac{\partial\lambda}{\partial t} + \boldsymbol{u} \cdot \nabla(\lambda) = \frac{1}{t_{eq}} \left[(1-\lambda) - (1-\lambda_{eq}) \left(\frac{\lambda}{\lambda_{eq}} \right) \right] \tag{6}$$

where the RHS is composed of a (positive) buildup term and a (negative) breakdown term de Souza Mendes (2009). The parameter t_{eq} is the equilibrium time, which physically means a time scale for the microstructure buildup process. It can be easily observed that when $t_{eq} \to 0$ the fluid structure instantaneoulsy develops to its equilibrium state and no thixotropic behavior is observed. This situation result in a purely elasto-viscous behavior, and is the situation analyzed in the present work. The relation between the equilibrium structure parameter, λ_{eq}, and the equilibrium viscosity η_{eq} (or the steady state viscosity, obtained in the flow curve) is given by:

$$\lambda_{eq}(\dot{\gamma}) = \frac{\ln \eta_{eq}(\dot{\gamma}) - \ln \eta_\infty}{\ln \eta_o - \ln \eta_\infty} \tag{7}$$

where η_o is the zero-shear-rate viscosity and $\dot{\gamma} \equiv \sqrt{\frac{1}{2} \operatorname{tr} \dot{\boldsymbol{\gamma}}^2}$ is the intensity of $\dot{\boldsymbol{\gamma}}$. The equilibrium structure parameter λ_{eq} is a scalar quantity that varies within the range $[0, 1]$. It gives a measure of the structuring level of the microstructure: $\lambda_{eq} = 0$ when the structuring level is minimum, and $\lambda_{eq} = 1$ when the material is fully structured. The equilibrium structure parameter λ_{eq} can thus be seen as a normalized equilibrium viscosity function, since there is a one-to-one relationship between structure and viscosity levels.

The relaxation and retardation times are defined as

$$\theta_1 = \left(1 - \frac{\eta_\infty}{\eta_{eq}} \right) \frac{\eta_{eq}}{G_{eq}} \tag{8}$$

ISSN 2176-5480

$$\theta_2 = \left(1 - \frac{\eta_\infty}{\eta_{eq}}\right)\frac{\eta_\infty}{G_{eq}} \tag{9}$$

where η_∞ is the infinite-shear-rate viscosity, and G_{eq} is the equilibrium elastic modulus ((de Souza Mendes and Thompson, 2012b)):

$$G_{eq} = G_o e^{m\left(\frac{1}{\lambda_{eq}}-1\right)} \tag{10}$$

In this equation, G_o is the structural elastic modulus of the fully structured material, and m is a positive scalar parameter that dictates the sensitivity of G_{eq} with λ_{eq}. It can be observed that its lowest value (i.e., highest relaxation and retardations times) occurs at the highest value of λ, and it increases as λ decays. This function is chosen to simulate the elastic behavior of viscoplastic fluids at the regions of low stress values, i.e., where the stress is below the yield stress.

The equilibrium viscosity ((de Souza Mendes and Dutra, 2004)) is chosen to represent the viscoplastic behavior of the fluid:

$$\eta_{eq}(\dot\gamma) = \left[1 - \exp\left(-\frac{\eta_o\dot\gamma}{\tau_y}\right)\right]\left\{\frac{\tau_y}{\dot\gamma} + K\dot\gamma^{n-1}\right\} + \eta_\infty \tag{11}$$

In this equation, τ_y is the yield stress, K the consistency index, and n the power-law index.

The fluid behavior is characterized by three different regions in the flow curve, namely the end of the highest viscosity plateau $\dot\gamma_o$, the begining of the power law viscosity behavior $\dot\gamma_1$, and the begining of the lowest viscosity plateau $\dot\gamma_2$:

$$\dot\gamma_o = \frac{\tau_y}{\eta_o}\ , \quad \dot\gamma_1 = \left(\frac{\tau_y}{K}\right)^{1/n}\ , \quad \dot\gamma_2 = \left(\frac{\eta_\infty}{K}\right)^{1/n-1} \tag{12}$$

where η_0 is the low shear rate viscosity plateau, τ_y is the yield stress, K is the consistency index, n is the power-law index, and η_∞ is the high shear rate viscosity plateau.

2.1 Dimensionless parameters

The dimensionless parameters are obtained using the scaling procedure proposed by (de Souza Mendes, 2007):

$$\begin{aligned} &t^* = t\dot\gamma_1\ ; \quad \boldsymbol{x}^* = \frac{\boldsymbol{x}}{R}\ ; \quad \boldsymbol{u}^* = \frac{\boldsymbol{u}}{\dot\gamma_1 R}\ ; \ \dot\gamma^* = \frac{\dot\gamma}{\dot\gamma_1}\ ; \\ &P^* = \frac{P}{\tau_y}\ ; \quad \boldsymbol{\tau}^* = \frac{\boldsymbol{\tau}}{\tau_y}\ ; \quad \eta^*_{eq} = \frac{\eta_{eq}\dot\gamma_1}{\tau_y} \end{aligned} \tag{13}$$

The governing dimensionless equations for non-thixotropic, steady creeping flows are given by:

$$\nabla^*\cdot\boldsymbol{u}^* = 0 \qquad \text{in } \Omega^* \tag{14}$$

$$\nabla^*\cdot\boldsymbol{\tau}^* - \nabla^* P^* = \mathbf{0} \qquad \text{in } \Omega^* \tag{15}$$

$$\boldsymbol{\tau}^* + \theta_1^*(\lambda)\check{\boldsymbol{\tau}}^* = 2\eta_v^*(\lambda)\left[\dot{\boldsymbol{\gamma}}^* + \theta_2^*\overset{\triangledown}{\dot{\boldsymbol{\gamma}}}\right] \qquad \text{in } \Omega^* \tag{16}$$

$$\lambda = \lambda_{eq} \qquad \text{in } \Omega^* \tag{17}$$

where $\dot{\boldsymbol{\gamma}}^* = \frac{1}{2}\left(\nabla^*\boldsymbol{u}^* + \nabla^*\boldsymbol{u}^{*T}\right)$, and $\check{\boldsymbol{\tau}}^* = (\nabla^*\boldsymbol{\tau}^*)\cdot\boldsymbol{u}^* - (\nabla^*\boldsymbol{u}^*)\cdot\boldsymbol{\tau}^* - \boldsymbol{\tau}^*\cdot(\nabla^*\boldsymbol{u}^*)^T$. The dimensionless viscosity, relaxation and retardation times are given by:

$$\eta^*_{eq}(\dot\gamma^*) = [1 - \exp(-(J+1)\dot\gamma^*)]\left(\frac{1}{\dot\gamma^*} + \dot\gamma^{*(n-1)}\right) + \eta^*_\infty \tag{18}$$

$$\theta_1^*(\dot\gamma^*) = \alpha\frac{\eta^*_{eq}}{G_0^*} \qquad \theta_2^*(\dot\gamma^*) = \alpha\frac{\eta^*_\infty}{G_0^*} \tag{19}$$

where

$$\alpha = \frac{(1-\eta^*_\infty)}{\exp\left(\mathrm{m}(1/\lambda_{\mathrm{eq}} - 1)\right)} \tag{20}$$

ISSN 2176-5480

3. NUMERICAL MODELING

The numerical solution is obtained via the finite element method, using a four-field Galerkin least-squares (GLS) formulation, in terms of the structure parameter, velocity, pressure and extra-stres. The GLS method produces stable approximations for both elastic- and viscous- dominated flow regions, using simple combinations of finite element interpolations, and allowing the use of equal-order combinations of Lagrange finite elements ((**?**)).

The numerical formulation is described in details in (Fonseca *et al.*, 2012). It employs the usual finite element subspaces for incompressible multi-field problems: $\lambda \in H^1(\Omega)$, $\boldsymbol{\tau} \in C^0(\Omega)^{N\times N} \cap H^2(\Omega)^{N\times N}$, $P \in C^0(\Omega) \cap L_2^0(\Omega)$ and $\boldsymbol{u} \in H^1(\Omega)^N$, and uses stability parameters to control the conservation, constitutive , and evolution equations. The discretization of the GLS formulation results in a non-linear system of equations, which is solved using a quasi-Newton method (see (**?**) for details).

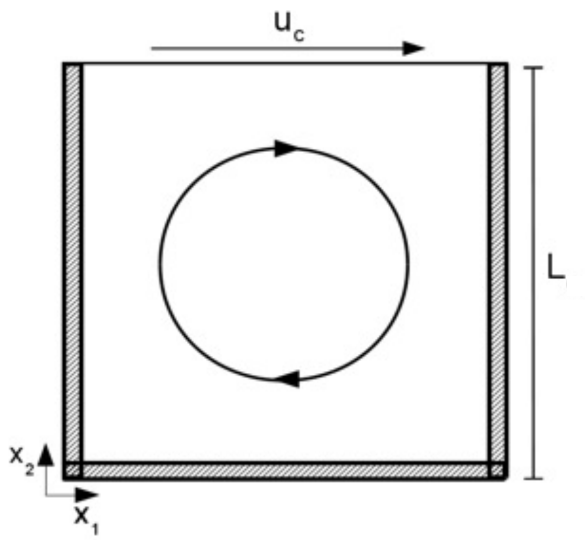

Figure 1. The geometry and boundary conditions

The geometry analyzed is a quadratic cavity of length L, as depicted in Fig. 1. The tap wall is subjected to a horizontal velocity u_c from left to right, along with no-slip and impermeability conditions. Therefore, $\mathbf{u} = u_c\,\mathbf{e_1}$ at the tap wall, and $\mathbf{u} = \mathbf{0}$ on the remaining walls. All results are obtained using an equal-order of bi-linear (Q1) finite element interpolation. A mesh independence procedure evaluating the relative error of the extra-stress magnitude is performed. Fig. 2 shows a detailed view of the stress profile at $x_1^* = 0.5$. Despite results are almost coincident for the meshes investigated (errors below 3%), the more refined mesh tested – with 100 $Q1$ finite elements and 10,201 nodal points.

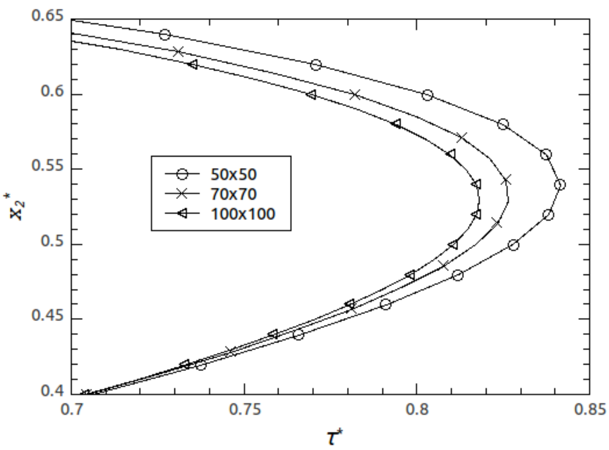

Figure 2. Comparison of the stress module ($\tau = \sqrt{1/2\mathrm{tr}\boldsymbol{\tau}^2}$) for three different meshes.

ISSN 2176-5480

4. RESULTS AND DISCUSSION

The results are obtained for steady flows, neglecting inertia and thixotropy. All the results are obtained for $\eta^*_\infty = 0.01$. The results show the effects of the rheological parameters and of the lid cavity velocity on the yield surfaces. The yield surfaces are defined as the locus of points in which the magnitude of the strain rate is below the lowest shear rate value for which the viscosity equals the higher viscosity plateau where $\eta = \eta_0$, i.e., when $\dot{\gamma} \leq \dot{\gamma}_0$ ((dos Santos *et al.*, 2011)).

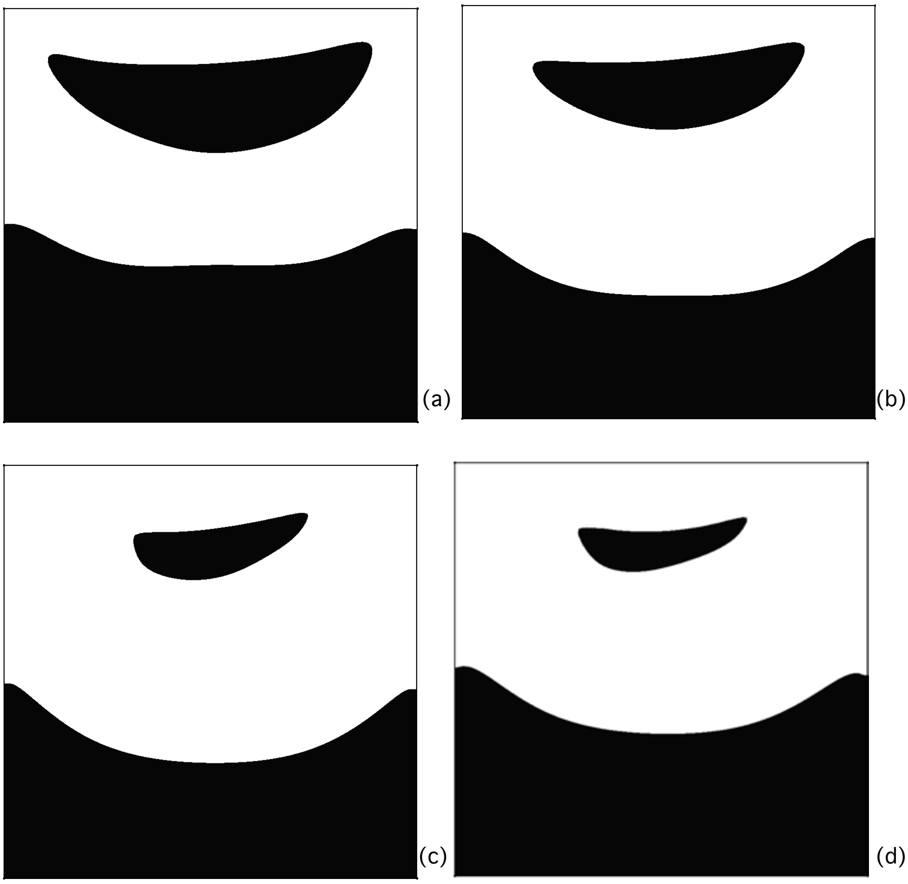

Figure 3. Yield surfaces: Effect of the jump number - high elasticity: $G_0^* = 7$, $n = 0.5$ and $U^* = 0.01$, and (a)$J = 500$; (b)$J = 1000$; (c)$J = 5000$; (d)$J = 10000$.

Figure 3 show the influence of the jump number J on the topology of yield surfaces, for $U^* = 0.01$, $n = 0.5$, and $G_0^* = 7$. The black regions represent the unyielded zones ($\dot{\gamma} < \dot{\gamma}_0$), while the white regions represent the yielded zones. As fluid elasticity increases (higher relaxation time, $G_0^* = 7$, Fig. 3), It can be observed that there are two unyielded zones, one symmetric, attached to the bottom wall and another one, non-symmetric, closer to the upper wall, located in the core of a flow recirculating zone. The bottom unyielded region is mildly affected by the Jump number, but the upper one strongly decreases as the Jump number increases. Elasticity is stronger inside the unyielded regions. Its effect is to increase the stress levels and the deformation rates, which in turn reduces the size of the unyielded regions. It is worth mentioning that the non symmetric flow pattern generated by elasticity was also observed in Nassar et al. (2007), in an expansion/contraction flow.

The effect of the lid cavity velocity is shown in Fig. 4 for $J = 500$, $n = 0.5$, and $G_0^* = 7$. As expected, increasing the lid velocity (which is equivalent to decrease the yield stress) leads to smaller (upper and bottom) unyielded regions due to higher levels of velocities and consequently, higher deformation rates as well. Again, due to elasticity (recall that there is no inertia), the flow pattern is non symmetric and the stress and strain levels are higher.

Figure 5 shows the effect of the power-law index. It can be observed that the flow pattern is almost insensitive to the power-law index. Increasing n leads to an increase in viscous effects, which tends to cancel out the elastic effect and turn the flow symmetric again.

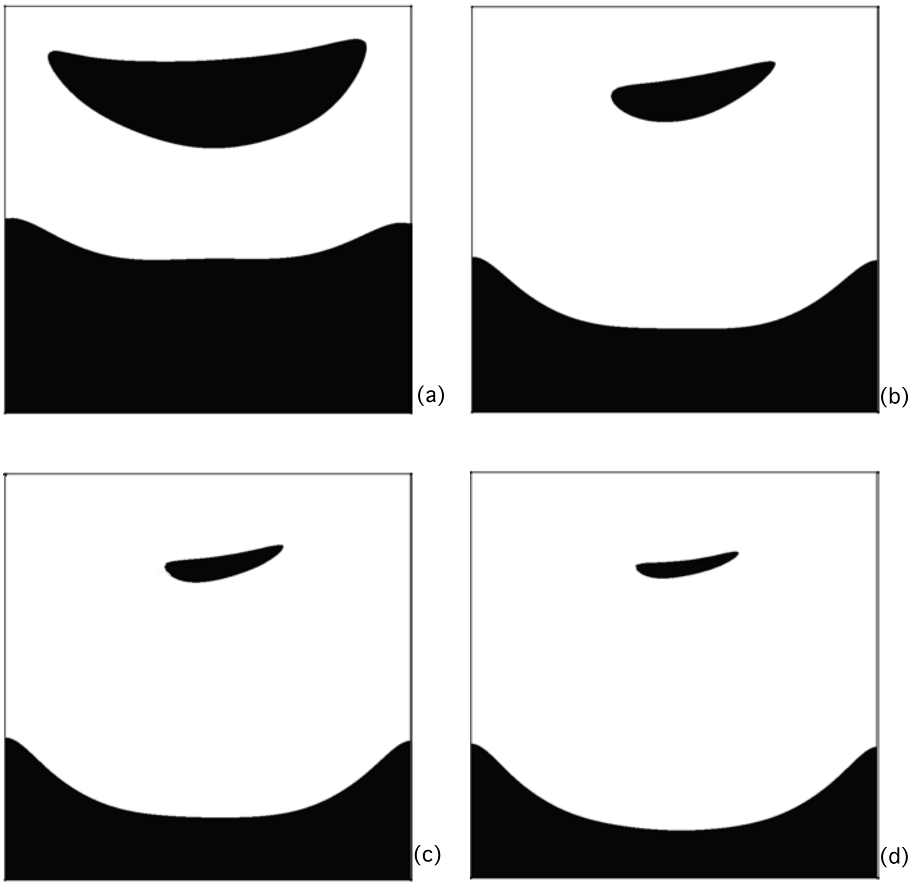

Figure 4. Yield surfaces: Effect of lid velocity for $n = 0.5$, $J = 500$ and $G_0^* = 7$, and (a)$U = 0.01$; (b)$U = 0.05$; (c)$U = 0.1$; and (d)$U = 0.15$.

5. FINAL REMARKS

Numerical simulations of inertialess flows of elasto-viscoplastic fluids have been undertaken in this article. The elasto-viscoplastic model used is the one introduced by de Souza Mendes (2011). The mechanical model is approximated by means of a four-field Galerkin least-squares method in extra-stress, pressure, velocity and the structure parameter. The numerical results have evidenced the influence of elasticity, shear-thinning, and viscoplastic nature of the material on the size and location of unyielded material regions. Elasticity showed to be crucial to better characterize the mechanical response of some viscoplastic materials.

6. ACKNOWLEDGEMENTS

The authors L. Hermany and D. Dall'Onder dos Santos thank for their graduate scholarships provided by CAPES and S. Frey, M.F. Naccache and P.R. de Souza Mendes acknowledges CAPES and CNPq for financial support.

7. REFERENCES

Alexandrou, A.N., Duc, E. and Entov, V., 2001a. "Inertial, viscous and yield stress effects in bingham fluid lling of a 2-d cavity". *J. Non-Newtonian Fluid Mechanics*, Vol. 96, pp. 383–403.

Alexandrou, A.N., McGilvreay, T.M. and Burgos, G., 2001b. "Steady Herschel-Bulkley fluid flow in three-dimensional expansions". *J. Non-Newtonian Fluid Mech.*, Vol. 100, pp. 77–96.

Barnes, H.A., 1997. "Thixotropy—a review". *J. Non-Newtonian Fluid Mech.*, Vol. 70, pp. 1–33.

Barnes, H.A., 1999a. "A brief history of the yield stress". *Appl. Rheology*, Vol. 9, pp. 262–266.

Barnes, H.A., 1999b. "The yield stress—a review". *J. Non-Newt. Fluid Mech.*, Vol. 81, pp. 133–178.

Bercovier, M. and Engelman, M., 1980. "A finite-element method for incompressible non-Newtonian flows". *J. Computat. Phys.*, Vol. 36, pp. 313–326.

Besses, D.D.D., Magnin, A. and Jay, P., 2003. "Viscoplastic flow around a cylinder in an infinite medium". *J. Non-Newtonian Fluid Mechanics*, Vol. 115, pp. 27–49.

Burgos, G.R. and Alexandrou, A.N., 1999. "Flow development of Herschel-Bulkley fluids in a sudden 3-d expansion". *J.*

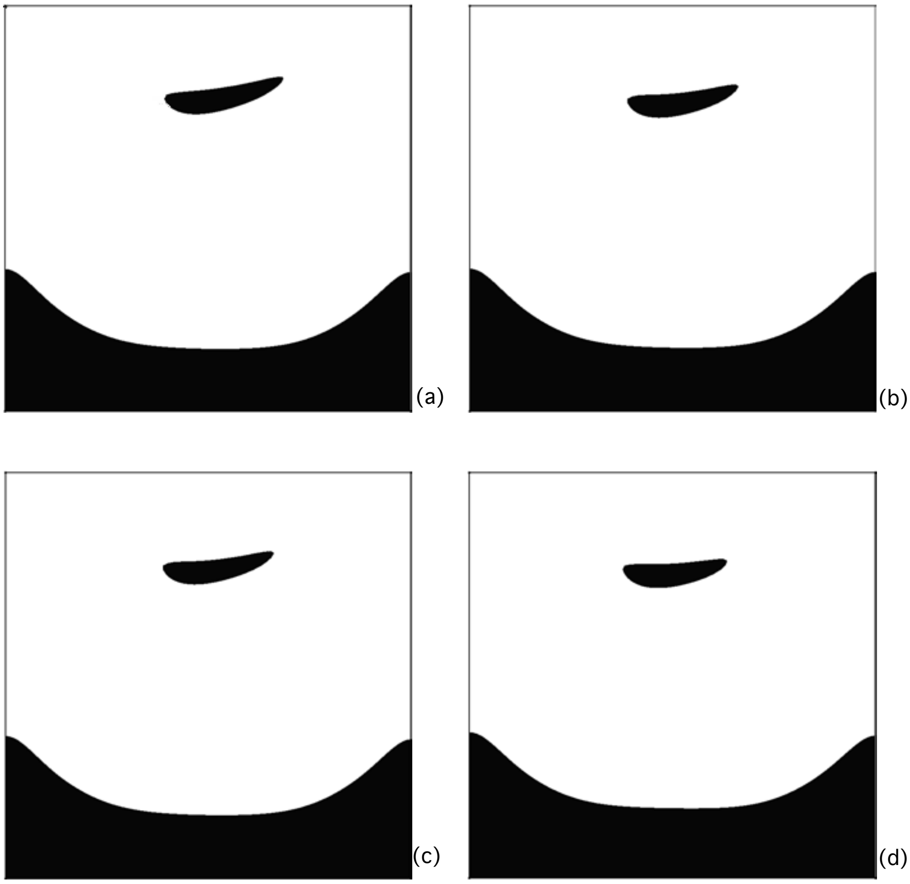

Figure 5. Yield surfaces: Effect of the power-law index for $G_0^* = 7$, $J = 500$ and $U^* = 0.1$, and (a)$n = 0.5$; (b)$n = 0.7$; (c)$n = 0.9$; (d)$n = 1.0$.

Rheology, Vol. 43, No. 3, pp. 485–489.

Burgos, G., Alexandrou, A. and Entov, V., 1999. "On the determination of yield surfaces in Herschel–Bulkley fluids". *J. Rheol.*, Vol. 43, No. 3, pp. 463–483.

Carter, R.E. and Warren, R.C., 1987. "Extrusion stresses, die swell, and viscous heating effects in doublebase propellants". *J. Rheology*, Vol. 31, pp. 151–173.

de Souza Mendes, P.R., 2007. "Dimensionless non-newtonian fluid mechanics". *J. Non-Newtonian Fluid Mechanics*, Vol. 147, pp. 109–116.

de Souza Mendes, P.R., 2009. "Modeling the thixotropic behavior of structured fluids". *J. Non-Newtonian Fluid Mech.*, Vol. 164, pp. 66–75. doi:doi:10.1016/j.jnnfm.2009.08.005.

de Souza Mendes, P.R., 2011. "Thixotropic elasto-viscoplastic model for structured fluids". *Soft Matter*, Vol. 7, pp. 2471–2483. doi:10.1039/c0sm01021a.

de Souza Mendes, P.R. and Dutra, E.S.S., 2004. "Viscosity function for yield-stress liquids". *Applied Rheology*, Vol. 14, No. 6, pp. 296–302.

de Souza Mendes, P.R., Naccache, M.F., Varges, P.R. and Marchesini, F.H., 2007. "Flow of viscoplastic liquids through axisymmetric expansions-contractions". *J. Non-Newtonian Fluid Mech.*, Vol. 142, No. 1-3, pp. 207–217.

de Souza Mendes, P.R. and Thompson, R.L., 2012a. "A critical overview of elasto-viscoplastic thixotropic modeling". *Journal of Non-Newtonian Fluid Mechanics*, Vol. 187, pp. 8–15.

de Souza Mendes, P.R. and Thompson, R.L., 2012b. "A unified approach to model elasto-viscoplastic thixotropic yield-stress materials and apparent-yield-stress fluids". *J. Rheol.*, Vol. submitted.

dos Santos, D., Frey, S., Naccache, M. and de Souza Mendes, P., 2011. "Numerical approximations for flow of viscoplastic fluids in a lid-driven cavity". *Journal of Non-Newtonian fluid mechanics*, Vol. 166, pp. 667–679.

Fonseca, C., Frey, S., Naccache, M.F. and de Souza Mendes, P.R., 2012. "Flow of an elasto-viscoplastic thixotropic fluid past a confined cylinder". *J. Non-Newtonian Fluid Mechanics*, Vol. (article in press).

Hammad, K.J., Vradis, G.C. and Ötügen, M.V., 2001. "Laminar flow of a Herschel-Bulkley fluid over an axisymmetric sudden expansion". *J. Fluids Engineering*, Vol. 123, pp. 588–594.

Liu, B.T., Muller, S.J. and Denn, M.M., 2002. "Convergence of a regularization method for creeping flow of a Bingham material about a rigid sphere". *J. Non-Newtonian Fluid Mech.*, Vol. 102, pp. 179–191.

Martins, R.R., Furtado, G.M., dos Santo, D.D., Frey, S., Naccache, M.F. and de Souza Mendes, P.R., 2013. "Elastic and viscous elastic e ects on ow pattern of elasto-viscoplastic uids in a cavity". *Mechanics Research Communications*, Vol. (submitted).

Mewis, J., 1979. "Thixotropy - a general review". *J. Non-Newtonian Fluid Mech.*, Vol. 6, pp. 1–20.

Mewis, J. and Wagner, N.J., 2009. "Thixotropy". *Adv Colloid Interface Sci*, Vol. 147-148, pp. 214–227.

Mitsoulis, E., Abdali, S.S. and Markatos, N.C., 1993. "Flow simulation of Herschel-Bulkley fluids through extrusion dies". *J. Non-Newtonian Fluid Mechanics*, Vol. 71, pp. 147–160.

Mitsoulis, E., Marangoudakis, S., Spyratos, M. and Zisis, T., 2006. "Pressure-driven flows of Bingham plastics over a square cavity". *J. Fluids Engineering*, Vol. 128, pp. 993–1003.

Naccache, M.F. and Barbosa, R.S., 2007. "Creeping flow of viscoplastic materials through a planar expansion followed by a contraction". *Mechanics Research Communications*, Vol. 34, pp. 423–431.

Nassar, B., de Souza Mendes, P.R. and Naccache, M.F., 2011. "Flow of elasto-viscoplastic liquids through an axisymmetric expansion–contraction". *J. Non-Newtonian Fluid Mechanics*, Vol. 166, pp. 386–394.

Papanastasiou, T.C., 1987. "Flows of materials with yield". *J. Rheology*, Vol. 31, pp. 385–404.

Roquet, N. and Saramito, P., 2003. "An adaptive finite element method for Bingham fluid flows around a cylinder". *Comput. Methods Appl. Mech. Eng.*, Vol. 192, pp. 3317–3341.

Saramito, P., 2007. "A new constitutive equation for elastoviscoplastic fluid flows". *J. Non-Newt. Fluid Mech.*, Vol. 145, pp. 1–14.

Sikorski, D., Tabuteau, H. and de Bruyn, J.R., 2009. "Motion and shape of bubbles rising through a yield-stress fluid". *J. Non-Newtonian Fluid Mech.*, Vol. 159, pp. 10–16.

Sofou, S., Muliawan, E.B., Hatzikiriakos, S.G. and Mitsoulis, E., 2008. "Rheological characterization and constitutive modeling of bread dough". *Rheol. Acta*, Vol. 47, pp. 369–381.

Zisis, T. and Mitsoulis, E., 2002. "Viscoplastic flow around a cylinder kept between parallel plates". *J. Non-Newtonian Fluid Mech.*, Vol. 105, pp. 1–20.

8. RESPONSIBILITY NOTICE

The authors are the only responsible for the printed material included in this paper.